JMEPEG (2023) 32:6564–6575
https://doi.org/10.1007/s11665-022-07581-y

1059-9495/$19.00

TECHNICAL ARTICLE

Effects of Isothermal Solution Treatment on Microstructure Evolution and Tensile Properties of High Strength Near-β Ti Alloy

Bo Song, Wenlong Xiao, Chaoli Ma, and Lian Zhou

Submitted: 6 July 2022 / Revised: 7 October 2022 / Accepted: 14 October 2022 / Published online: 1 November 2022

The influence of slow cooling rate and the isothermal holding temperature in isothermal solution treatment on microstructure evolution and tensile properties of near-β Ti alloy was investigated in this work. The results showed that plenty of colonies consisting of parallel α needles were formed during the slow cooling and the isothermal holding stages. In comparison with the primary α developed during solutionizing, the secondary α precipitates formed during aging were more effective in strengthening the alloy. The hardness difference observed due to the cooling rate changes was reduced as the isothermal solutionizing temperature was increased. With the isothermal holding temperature decreasing, the volume fraction of primary α was gradually increased, and the volume fraction of secondary α precipitates dropped accordingly. When held below 750 °C, basketweave microstructures could be obtained after aging treatment, because most of α phase had been formed upon solution stage with plate-like shape. These α plates could accommodate larger degree of local strain than secondary α precipitates, resulting in higher fracture elongation of alloy. A balanced combination of strength and ductility was achieved under the cooling rate of 10 °C/min and isothermal holding temperature of 800 °C, and the yield strength, ultimate tensile strength, elongation and area reduction were 1470, 1497 MPa, 4 and 5.8%, respectively.

Keywords isothermal solution plus aging treatment, mechanical properties, microstructures evolution, titanium alloy

1. Introduction

Near β titanium alloys have been widely used in aerospace industry due to their excellent properties, such as high specific strength, deep hardenability and good corrosion resistance (Ref 1, 2). These properties are mainly determined by the transformation of secondary phase in β matrix, which can produce great precipitation hardening effect. It has been widely acknowledged that the morphology, size, number density and distribution of α precipitates can greatly influence mechanical properties of near-β Ti alloy. Through tailoring these features of α precipitates, the combination of strength and ductility can be changed in a wide range (Ref 3-6). Various heat treatments have been employed to control the precipitation behavior of α phase, including double-aging treatment and slow heating to aging temperatures. It has been reported in the literature that the parameters of heat treatment, i.e., temperature / time, heating rate, cooling rate and aging methods, can greatly affect the precipitation of α phase, and lead to the alloy obtained different properties (Ref 7-12). This is mainly due to these heat treatment parameters can change nucleation and growth pathways of α precipitates (Ref 13, 14).

High ductility and superior fracture toughness are generally obtained by developing α lamellars, but at this time the alloy shows comparatively low strength. In comparison with α lamellars, the combination of strength and ductility can be obviously improved by developing heterogeneous α precipitates, which is composed of not only lamellar α phase having large aspect ratio but also short-rod shape α precipitates with nanoscale size (Ref 15-17). Jiang et al. (Ref 18) showed the formation of heterogeneous α phase in Ti-15Mo-3Al-2.7Nb-0.2Si alloy by high and low temperatures two-step aging, and an excellent match between strength and ductility was obtained. Shekhar et al. (Ref 8) also reported mixed microstructure consisting of α precipitates with heterogeneous size as well as an optimum combination of strength and ductility. In titanium alloys, β annealing followed by slow cooling and aging (BASCA) treatment is originally developed to maximize their fracture toughness. Interestingly, it has been proven that titanium alloys can develop multiscale α phase with heterogeneous sizes (Ref 19-21). For example, the mixed microstructure containing α colonies, acicular α and discontinuous grain boundary α phases has been derived in Ti-4Al-7Mo-3Cr-3V alloy through BASCA heat treatment, leading to enhanced tensile properties (Ref 20). To our knowledge, higher strength can be achieved through decreasing aging temperatures. Therefore, an unconventional heat treatment is developed based on BASCA treatment in this work, in which an additional

Bo Song, School of Materials Science and Engineering, Liaocheng University, Liaocheng 252059 Shandong, China; and Key Laboratory of Aerospace Advanced Materials and Performance of Ministry of Education, School of Materials Science and Engineering, Beihang University, Beijing 100191, China; and **Wenlong Xiao, Chaoli Ma,** and **Lian Zhou**, Key Laboratory of Aerospace Advanced Materials and Performance of Ministry of Education, School of Materials Science and Engineering, Beihang University, Beijing 100191, China. Contact e-mails: songbo@lcu.edu.cn and wlxiao@buaa.edu.cn.

aging at lower temperature is performed after the BASCA procedure, referred as isothermal solution plus aging treatment. The main propose of such heat treatment is to further improve the combination of strength and ductility meanwhile maintaining superior fracture toughness.

Recently, a novel near-β Ti alloy Ti-5Al-3Mo-3V-2Cr-2Zr-1Nb-1Fe (wt.%, Ti-5321) was designed to use in high-strength aircraft components (Ref 22, 23). Depending on microstructures tailoring, the ultimate tensile strength, elongation and fracture toughness of Ti-5321 alloy can fluctuate in a range of 1147-1439 MPa, 3-26% and 57-114 MPa $m^{1/2}$, respectively. Wang et al. (Ref 21) have studied the evolution of three kinds of α lamellars in Ti-5321 alloy under BASCA treatments, as well as the according tensile properties. They found the texture intensity and variant selection degree of lamellar α phase was gradually increased during continuous cooling, and being closely related to the fracture behavior and tensile properties of alloy. However, researches on the formation and evolution of mixed microstructure in high-strength β-Ti alloy are still lack, which may achieve better combinations of strength and ductility than α lamellars.

In this work, the microstructure evolution in Ti-5321 alloy during isothermal solution plus aging treatment and their corresponding tensile properties have been studied. The influence of isothermal holding temperature and slow cooling rate from β zone to isothermal holding stage on the formation of plate-like primary α phase and secondary α precipitates were analyzed. The deformation and fracture behaviors of α precipitates with different characters were also discussed. It was suggested that the secondary α precipitates with short-rod shape was more efficient to strengthen alloy in comparison with the primary α plates.

2. Materials and Methods

The raw material Ti-5321 alloy was provided by Northwest Institute for Non-ferrous Metal Research, China (Ref 22). It was hot rolled in α + β phase field into ϕ 20 mm in diameter. The detailed chemical composition was Ti-5.02Al-3.03Mo-2.99V-2.06Cr-2.01Zr-1.37Nb-0.99Fe (wt.%), and its β transus temperature of this alloy was about 860 °C measured by metallographic method (Ref 23). The isothermal solution plus aging treatments in this work were performed with Ar protection. Firstly, the samples were solutionized at 900 °C for 0.5 h, and then these samples were slowly cooled to various targeted temperatures (i.e., 650, 700, 750, 800 and 830 °C) isothermally holding for 1 h followed by water quenching. Lastly, aging treatment was conducted at 600 °C for 8 h. During aging treatment the samples with thickness of 5 mm were heated to 600 °C at 10 °C/min. The slow cooling rates from 900 °C to targeted holding temperatures were selected as 2 and 10 °C/min. The procedure of isothermal solution plus aging treatments used in this work is schematically illustrated in Fig. 1, which could be divided into three stages, including the slow cooling stage, isothermal holding stage and final aging stage.

To study the microstructure evolution during heat treatment, interrupted experiments were conducted by water quenching when each stage finished. Standard Kroll's reagent (10 ml HF + 30 ml HNO_3 + 70 ml H_2O) was used to reveal the microstructures, which were observed by light microscopy (LM) and scanning electron microscopy (SEM). All SEM images were obtained in secondary electron SEM (SE-SEM) mode. The characteristics of α precipitates were measured by Image-Pro-Plus software, including length, thickness, volume fraction and number density. The phase constituents of samples were identified by means of x-ray diffraction (XRD). The microhardness was measured by Vickers method at a load of 300 gf for 15 s. Uniaxial tensile tests were carried out on an Instron 8801 testing system at a strain rate of 5×10^{-4} s^{-1}. Three tensile specimens with the gauge length of 18 mm were tested for each condition, and an extensometer was loaded to record deformation strain. Flat-shaped tensile specimen was employed with the thickness of 2 mm. In order to research the phase transformation upon aging at 600 °C, differential scanning calorimetry (DSC) measurements were conducted on Netzsch STA449F3 calorimeter using specimens of ∼ 20 mg at heating rate of 10 °C/min.

3. Results

3.1 Precipitation Hardening

Under the slow cooling rate of 2 °C/min, heat treatment was interrupted by water quenching to measure the microhardness of samples at the end of each stage, and the results are presented in Fig. 2(a). It showed that the hardness of alloy was gradually increased during heat treatment, and the according increasing rate was closely related to the isothermal holding temperature. It was thought that α phase would be formed upon three stages above, leading to precipitation hardening. With the isothermal holding temperature deceasing, the increasing rate of hardness values was gradually decreasing. For the isothermal holding temperature of 800 °C, the sample exhibited the largest increasing rate during heat treatment. It hardness value increased from 300 ± 6 to 400 ± 7 HV. When such temperature decreased to 700 °C, the hardness of sample only increased slightly from 330 ± 3 to 341 ± 2 HV.

After the slow cooling stage at the rate of 2 °C/min, the hardness of sample was increased with the ending temperature decreasing. The sample slowly cooled to 800 °C obtained hardness similar to that of β solution treated alloy (300 ± 5 HV). The sample slowly cooled to 700 °C showed the largest hardness. This should be due to the lower ending temperature provided longer time and larger driving force for α phase transformation, leading to more α phase formation and stronger hardening effect. When the isothermal holding stage finished, the sample held at 700 °C still had the largest hardness value, and the sample held at 750 and 800 °C obtained lower hardness. It should be noted that the hardness difference between various holding temperatures was apparently reduced in comparison with that at the end of slow cooling stage. Three samples have almost the same hardness value around 330 ± 5 HV. After aging stage, the hardness of sample held at 800 °C showed an abrupt increment to 400 ± 8 HV, and the hardness of sample held at 700 °C only slightly climbed up to 341 ± 2 HV. The microhardness of samples during heat treatment is summarized in Table 1.

Besides, it was found that the precipitation hardening behavior of α phase being dependent on the cooling rate from 900 °C to isothermal holding stage shown in Fig. 2(b). The samples at the cooling rate of 10 °C/min obtained larger

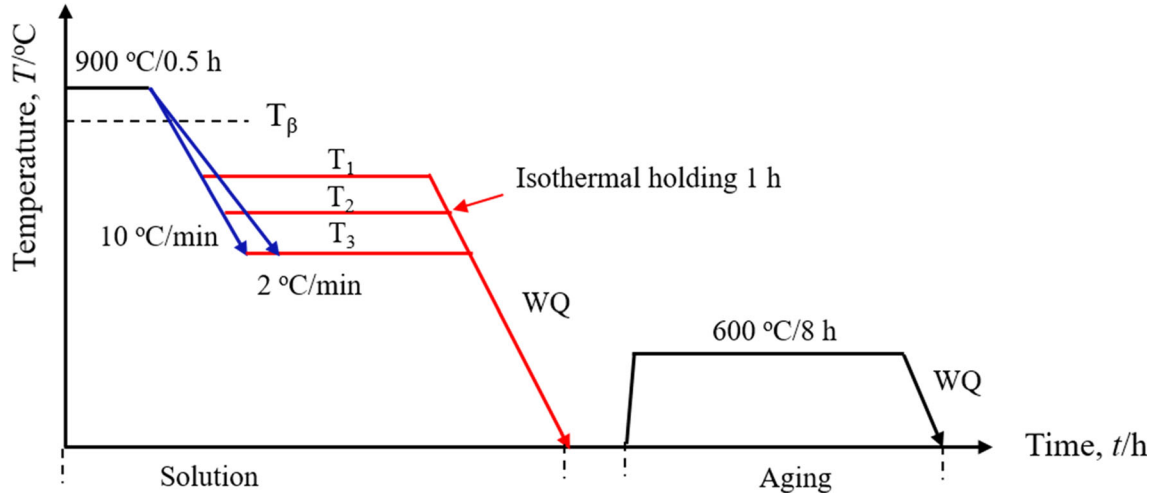

Fig. 1 Schematic diagram of the multiple heat treatments in this work

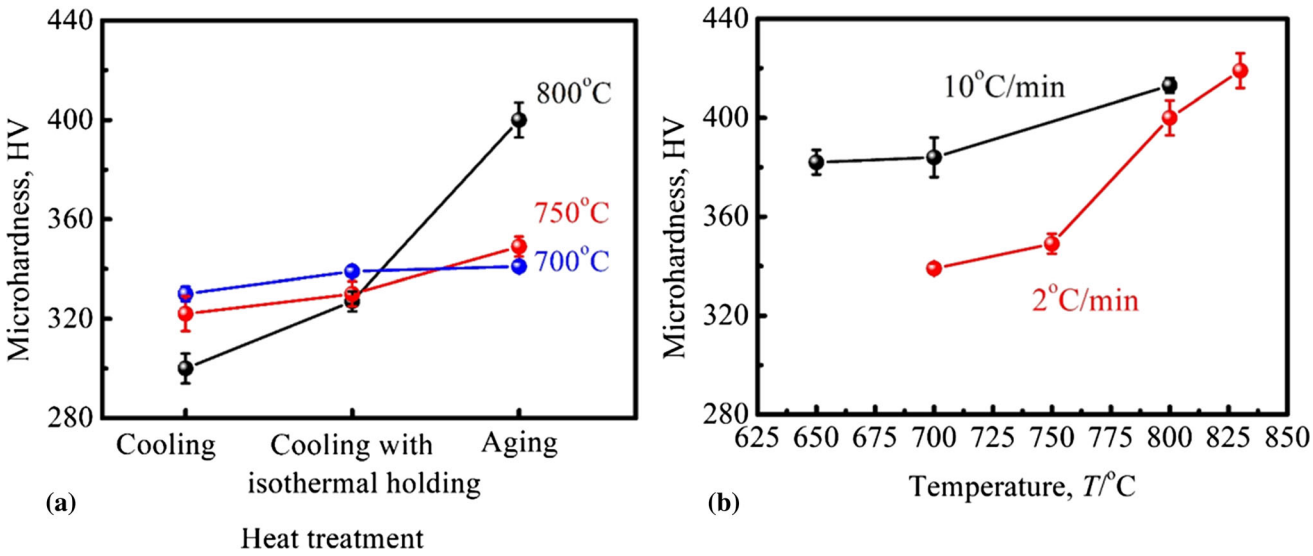

Fig. 2 Microhardness of Ti-5321 alloy during heat treatment at the cooling rate of 2 °C/min (a), and (b) the hardness difference in aged samples between 2 and 10 °C/min

Table 1 Microhardness of Ti-5321 alloy during heat treatment at different isothermal holding temperatures when cooled by 2 °C/min

	800 °C	750 °C	700 °C
Cooling	300 ± 6	322 ± 7	330 ± 3
Cooling and isothermal holding	327 ± 4	330 ± 5	339 ± 2
Aging	400 ± 8	349 ± 4	341 ± 2

hardness than that of 2 °C/min after aging treatment. The hardness difference between such two cooling rates was dropping gradually with the holding temperature increasing.

3.2 Microstructures Evolution

To explain the α precipitation hardening behavior in samples, the microstructures after each stage reserved by water quenching were carefully characterized, and the as-quenched microstructures are shown in Fig. 3. It was found that such isothermal holding temperature could greatly influence the characters of α precipitates. When the samples were cooled to comparable high temperatures, i.e., 830 and 800 °C, equiaxed β grains were visible shown in Fig. 3(a) and (b). The average diameter of β grains was measured to be 180 ± 20 μm, which should be determined by solution temperature and time. However, it was difficult to distinguish if there was primary α phase existence by LM observations. When isothermal the holding temperature decreased to 750 °C, plenty of α precipitates could be found clearly in β matrix shown in Fig. 3(c). The volume fraction of α phase was measured to be 25 ± 7%. The α precipitates in the sample slowly cooled to 750 °C showed two types of characteristics, some of them were formed along β grain boundaries forming grain boundaries α (GBα), and the others developed into colonies within grains, referred as intragranular α. Most of intragranular α were nucleated at β grain boundaries and grew into grains, and there was also α phase with low quantities formed initially in the grain interior.

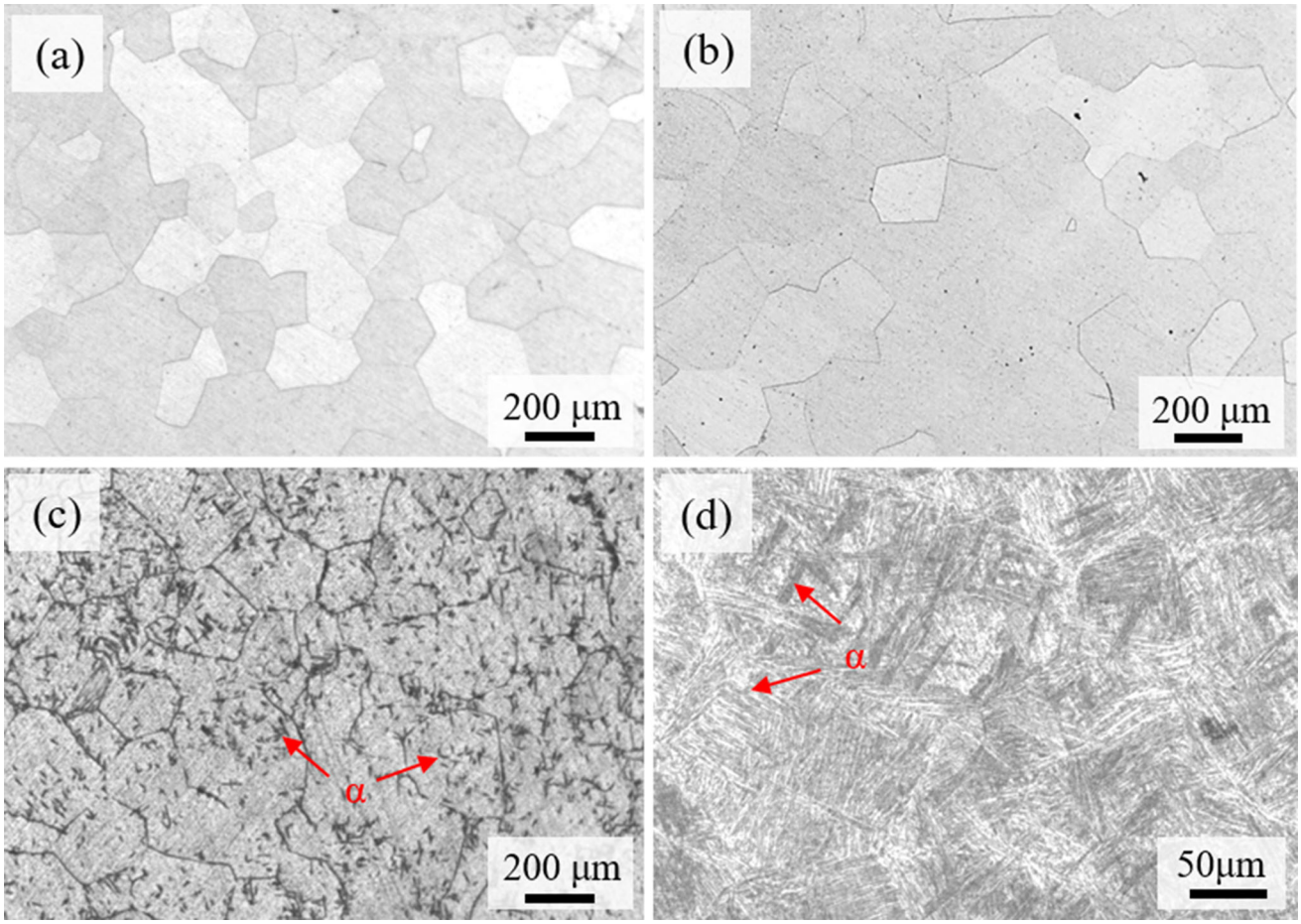

Fig. 3 Microstructures of Ti-5321 alloy slowly cooled to (a) 830 °C, (b) 800 °C, (c) 750 °C and (d) 700 °C from 900 °C at 2 °C/min

The nucleation sites for these α precipitates nucleated in grain interior may be dislocation enriched regions. In the sample cooled to 700 °C, typical basketweave structure was formed shown in Fig. 3(d). Plenty of colonies consisting of parallel α needles were visible.

When the samples were slowly cooled to 830 and 800 °C, the α phase should be formed in theory, because these temperatures are below the β transus temperature of Ti-5321 alloy. To study the formation of α phase, the phase constituents of samples were detected by XRD technology, and the results are given in Fig. 4. In the samples slowly cooled to 830 and 800 °C, the diffraction peaks from α phase were very weak but still could be identified, hence it was thought that α phase has been formed when the samples were slowly cooled to 830 and 800 °C. As the isothermal holding temperature decreased to 750 °C, the intensity of α phase peaks became stronger, indicating the increment of α phase quantities. This result was in according with LM observations above.

When the isothermal holding stage was completed, the samples were water quenched to room temperature. As shown in Fig. 5(a) and (b), plenty of colonies consisting of parallel α needles were formed within β grains after holding at 830 and 800 °C for 1 h. The quantities of α colonies in the sample held at 800 °C were apparently higher than that of 830 °C. It was due to the lower holding temperature provided larger driving force and accelerated α phase transformation. The features of α plates under different heat treatments are summarized in Table 2. After aging treatment, secondary α precipitates having short-rod shape and nanoscale size were formed besides α colonies. SEM images showing the features of such secondary α precipitates are presented in Fig. 5(c)-(f). Their characters were also greatly affected by the isothermal holding temperature. These fine secondary α precipitates in the sample held at 830 °C showed larger thickness and lower number density than that held at 800 °C. Under the holding temperature of 830 °C, the average thickness, length and number density of secondary α precipitates were 0.12 ± 0.02 μm, 0.34 ± 0.1 μm and 10 ± 4 laths/μm^2, respectively. In the sample held at 800 °C, their average thickness, length and number density were 0.07 ± 0.01 μm, 0.36 ± 0.12 μm and 15 ± 2 laths/μm^2, respectively. When the isothermal holding temperature decreased to 750 and 700 °C, the samples developed basketweave microstructures before aging shown in Fig. 6(a), (c), and α precipitates both exhibited plate-like shape. In the sample held at 750 °C, the number density of α phase grew up slightly after aging treatment (Fig. 6b). For the sample held at 700 °C, there was no apparent changes in microstructure characters after aging shown in Fig. 6(d).

Besides the isothermal holding temperature, the cooling rate from β zone to isothermal holding stage also produced great influence on the microstructures development, and resulted in different precipitation hardening effect. For the samples under the cooling rate of 2 °C/min, the corresponding microstructures have been studied above. When the cooling rate was increased to 10 °C/min, the microstructure evolution during heat treatment is presented in Fig. 7. Under the condition of holding

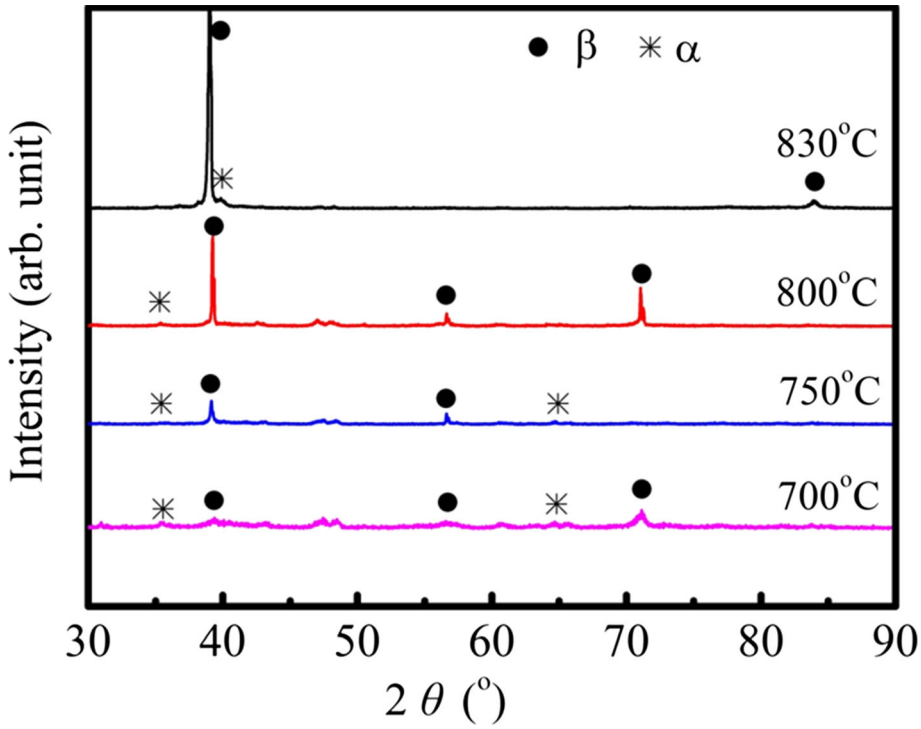

Fig. 4 XRD patterns of Ti-5321 alloy slowly cooled to different temperatures at 2 °C/min

temperature at 800 °C, equiaxed β grains were visible at the end of slow cooling stage shown in Fig. 7(a). XRD result also showed slight α phase diffraction peaks, indicating the presence of α phase, which was not shown here. There was still no apparent intragranular α at this time, and α phase may exist as GBα. When the isothermal holding stage at 800 °C was completed, intragranular α precipitates appeared within β grains and covered a volume fraction of 20 ± 5%. The GBα became more evident shown in Fig. 7(b). During the aging stage, quantities of secondary α precipitates were formed shown in Fig. 7(c), (d). The average thickness, length and number density of these secondary α precipitates were 0.1 ± 0.02 μm, 0.29 ± 0.1 μm and 16 ± 4 laths/μm^2, respectively. It was also noted that the secondary α precipitates nearby primary α plates exhibited needle-like shape. This indicated that the primary α phase would provide additional sites for the nucleation of secondary α precipitates.

When the isothermal holding temperature dropped to 750 °C, the microstructural features were apparently different between two cooling rates. Unlike typical basketweave microstructure formed at 2 °C/min, the size and number density of α colonies in samples cooled by 10 °C/min were obviously reduced shown in Fig. 7(e). In addition, some precipitation free zone (PFZ) was formed and developed into β blocks neighboring primary α plates. During the final aging treatment, α lamellas with same orientation originated from β grain boundaries and grew into grains, forming Widmanstatten structure. However, it was noted that there was still amounts of β transformed microstructure appearance shown in Fig. 7(f). This indicated that the secondary α precipitates could still be formed during aging.

3.3 Tensile Properties

Tensile properties of the samples after aging under different isothermal holding temperature and cooling rate conditions are presented in Fig. 8. When cooled by the same rate, the yield strength and ultimate tensile strength of alloy were decreased with the holding temperature dropping, while the ductility was greatly improved. For the slow cooling rate of 2 °C/min and isothermal holding temperature of 800 °C, the yield strength, ultimate tensile strength, elongation and area reduction of the sample after aging treatment reached to 1458 ± 15, 1494 ± 7 MPa, 4.4 ± 0.5 and 4.6 ± 1%, respectively. When the holding temperature dropped to 750 °C, the yield strength and ultimate tensile strength of alloy were decreased to 997 ± 5 and 1052 ± 9 MPa, but the elongation and area reduction were increased to 18.5 ± 2 and 25.1 ± 5%, respectively. Similar results were also found at the heating rate of 10 °C/min, in which the yield strength was decreased from 1470 ± 17 to 1179 ± 20 MPa with the holding temperature decreasing from 800 to 750 °C, and the elongation increased from 4.0 ± 1 to 16.7 ± 0.6%. The detailed strength and ductility of Ti-5321 alloy under various conditions are listed in Table 3. It deserved to be noted that the difference between two cooling rates was affected by the isothermal holding temperature. Under the holding temperature of 800 °C, the samples showed similar strength and ductility regardless of cooling rate. However, the differences in strength and ductility between two cooling rates were apparently broadened when such isothermal holding temperature dropped to 750 °C. This difference in yield strength was 23 MPa at holding temperature of 800 °C, and it reached to 182 MPa at holding temperature of 750 °C.

Typical fractographs of tensile specimen were selected to reveal the underlying fracture mechanisms controlling tensile properties. For the sample held at 800 °C after aging treatment, a mixture of intergranular and intragranular fracture characters could be found shown in Fig. 9(a), (b). Plain facets covering a low volume fraction were visible on the fracture surface, and many shallow dimples with a large area fraction were formed nearby these plain facets. This suggested that initial micro-

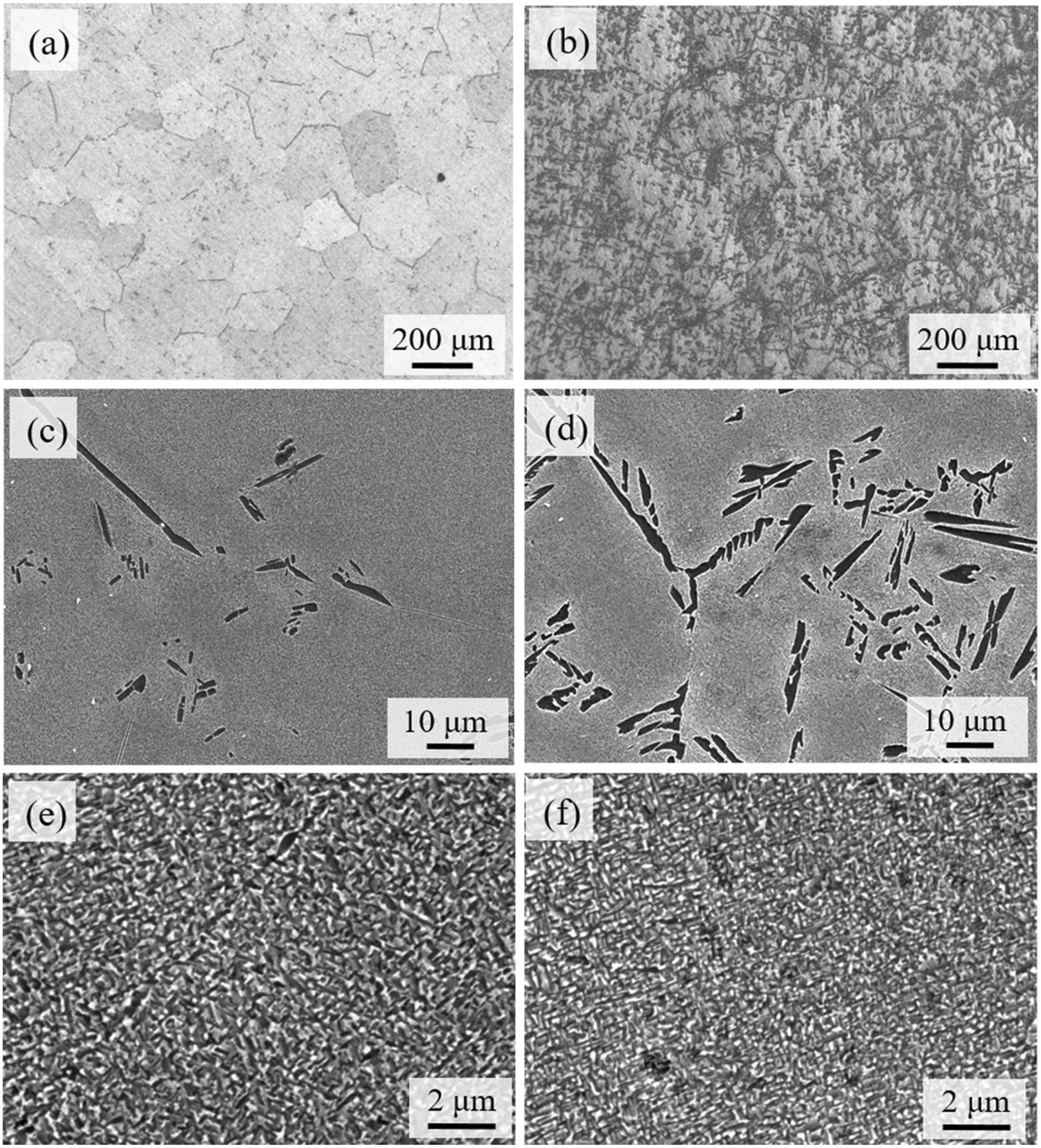

Fig. 5 Microstructures of the samples isothermally held at 830 °C (a) and 800 °C (b) for 1 h, and SEM images showing the aged microstructures of alloy held at (c, e) 830 °C and (d, f) 800 °C

Table 2 The features of primary α in samples before aging under different heat treatments

	Thickness, μm	Length, μm	Aspect ratio	Volume fraction, %
2 °C/min-800 °C	8.5 ± 3	32.2 ± 9	3.8 ± 2	29.8 ± 5
2 °C/min-750 °C	0.5 ± 0.2	20.4 ± 10	40.8 ± 6	53.3 ± 3
10 °C/min-800 °C	3.3 ± 1	21 ± 7	6.8 ± 5	20.8 ± 5
10 °C/min-750 °C	0.9 ± 0.3	29.2 ± 8	32.4 ± 10	44.8 ± 7

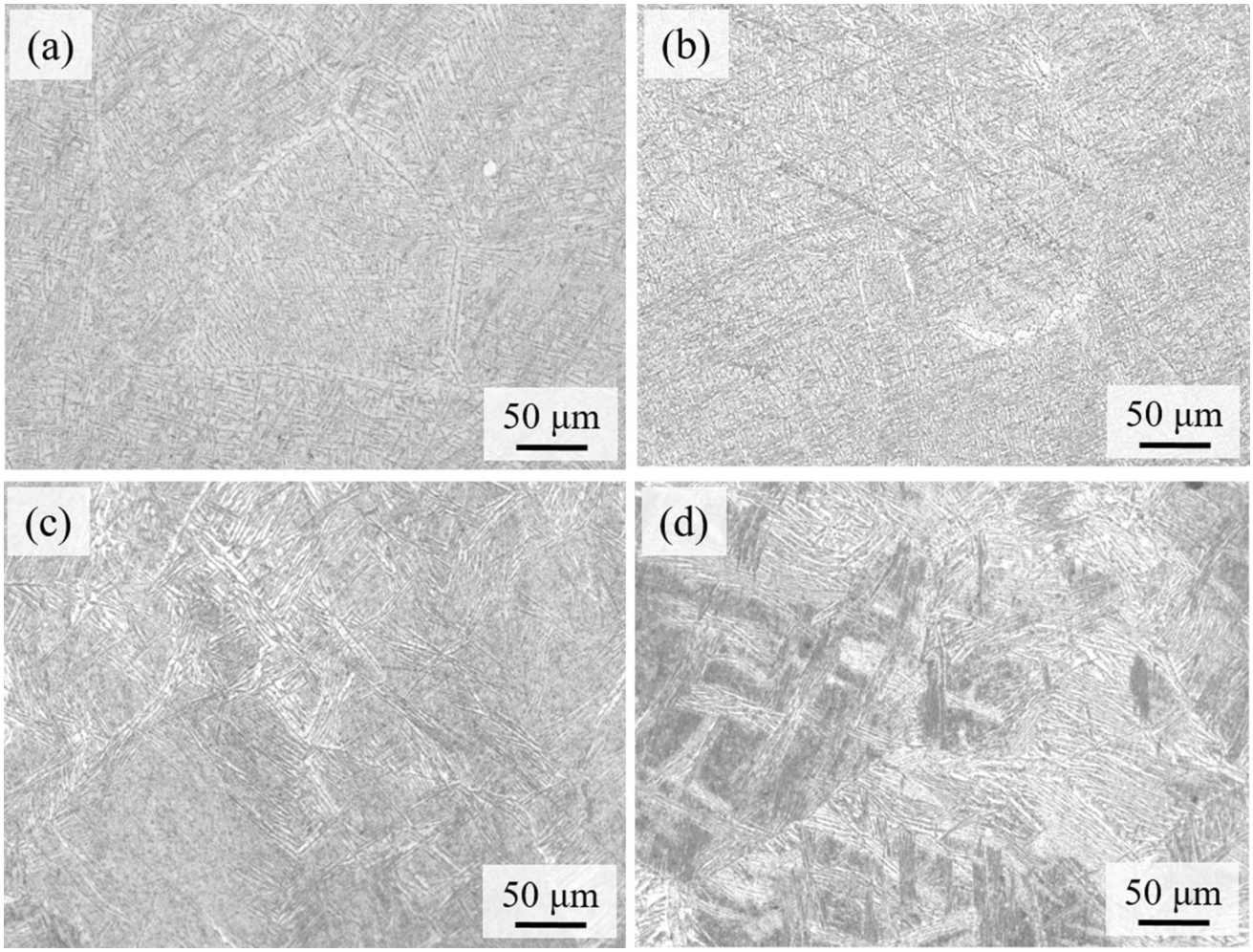

Fig. 6 LM images showing the microstructures of samples after isothermal holding at 750 °C (a) and 700 °C (c), and (b, d) corresponding microstructures after aging treatment

cracks were nucleated at two regions, i.e., the β grain boundaries and the interfaces between α and β phases. When the isothermal holding temperature dropped to 750 °C, a typical ductile fracture feature could be observed shown in Fig. 9(e), (f), and plenty of shallow and fine dimples were formed. It indicated that initial micro-cracks in this sample were mainly formed at the interfaces of α and β phases.

4. Discussion

The mechanical properties of near-β Ti alloys are primarily dominated by the morphology, size, number density and distribution of α precipitates; therefore, tailoring microstructure through heat treatment is crucial to improve mechanical properties of alloy. It has been found that mixed microstructure could be obtained using isothermal solution plus aging treatment in this study. The influence of the slow cooling rate to isothermal holding temperature and the following targeted holding temperature on the evolution of mixed microstructure and mechanical properties has been investigated. Based on the results above, the isothermal holding temperature produced a larger influence in comparison with the slow cooling rates. During heat treatment α phase was continuously formed, leading to apparent precipitation hardening effect. When such isothermal holding temperature was below 750 °C, the α phase would be transformed completely upon isothermal holding stage without secondary α development during aging, as evidenced by the microhardness and microstructures shown in Fig. 2(a) and 6.

When the isothermal holding temperature was higher than 750 °C, i.e., 830 and 800 °C, quantities of secondary α precipitates could be formed during aging. This was due to the retained β matrix was still unstable after the isothermal holding stage, and could further decompose upon aging. The α phase transformation behavior in β-solutionized Ti-5321 alloy during aging has been studied carefully and discussed in our previous work (Ref 24), and it was found that the secondary α was nucleated via O′-assisted mechanism (Ref 25, 26). The phase transformations in samples held at different temperatures have been examined in this work shown in Fig. 10. The phase transformation sequence under different holding temperatures was identical, even though the occurrence of phase transformations shifted to high temperatures with the holding temperature decreasing. The gray peaks were referred as the transformation of intermediate phases, such as O′, ω and O″ (Ref 24, 27, 28), and the black peaks were referred as the precipitation of α phase. This shift of phase transformation

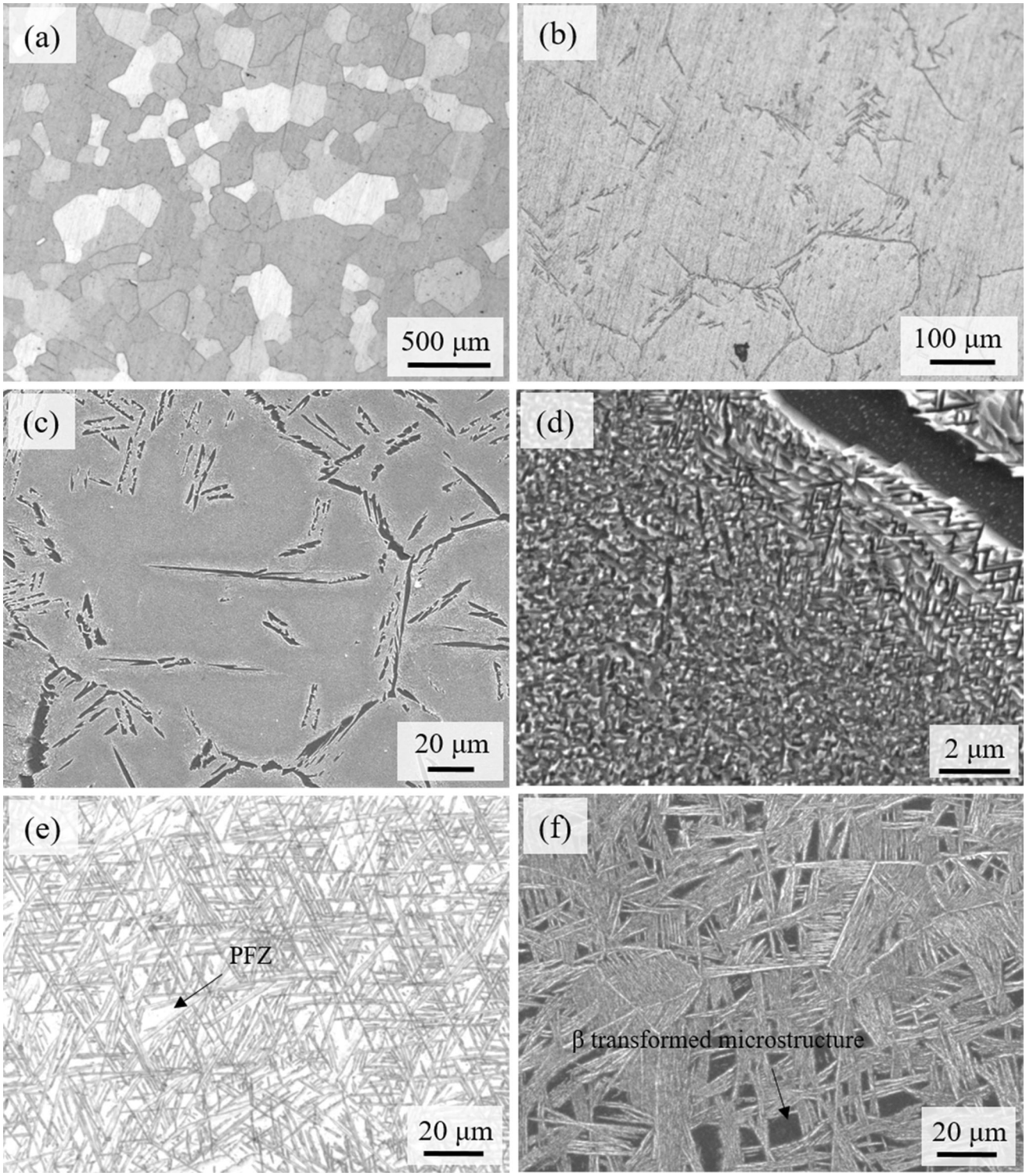

Fig. 7 Microstructures of the sample during heat treatment: (a) slowly cooling to 800 °C at 10 °C/min and (b) holding for 1 h, and SEM images (c, d) showing the microstructures after aging treatment. Optical images showing microstructures of alloy cooled to 750 °C at 10 °C/min holding for 1 h (e) and (f) after aging treatment

occurrence to high temperatures should be caused by the formation of primary α plates and the stronger stability of β matrix. As reported in the literature (Ref 6, 29), there was a compositional control between α precipitates and retained β matrix. During heat treatment α stabilizers would be concentrated in α phase, and β stabilizers, i.e., Mo, V and Cr, would be excluded and enriched in β matrix. Such partitioning of solute atoms could strengthen β matrix and weaken the driving force of α precipitation.

It was also noted that the microhardness increasing rate during three stages was different when the holding temperatures were higher than 750 °C, and the final aging produced stronger

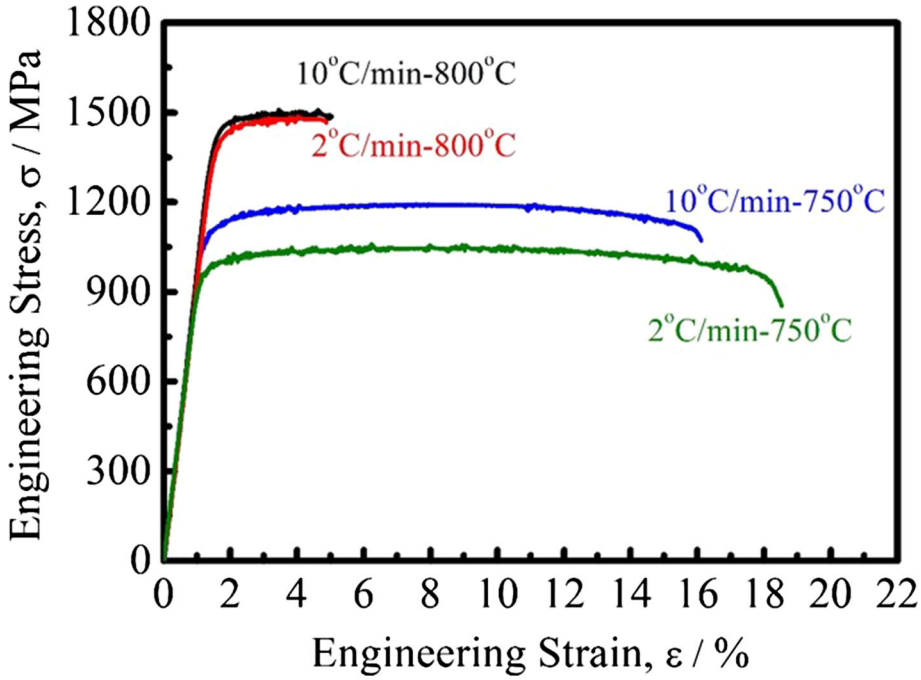

Fig. 8 Tensile curves of the aged alloy under various holding temperatures and cooling rates

Table 3 Tensile properties of Ti-5321 alloy after aging treatment in this work

	Yield strength, MPa	Ultimate strength, MPa	Elongation, %	Area reduction, %
2 °C/min-800 °C	1458 ± 15	1494 ± 7	4.4 ± 0.5	4.6 ± 1
2 °C/min-750 °C	997 ± 5	1052 ± 9	18.5 ± 2	25.1 ± 5
10 °C/min-800 °C	1470 ± 17	1497 ± 12	4.0 ± 1	5.8 ± 2
10 °C/min-750 °C	1179 ± 20	1200 ± 15	16.7 ± 0.6	22.6 ± 3

hardening effect (Fig. 2a). This was due to the secondary α precipitates were more effective to strengthen alloy than primary α plates with large thickness. Previous researches have studied that the deformation behavior of α phase with different characters, including large α plates and fine α particles (Ref 30, 31). When interacted with dislocations, the strength of α precipitates dependents on their size and exhibited size effect. The yield strength (σ_s) of α phase can be calculated by the equation $\sigma_s = k_\alpha \times d^{n1}$, in which the k_α and $n1$ are constants, d is the thickness of α precipitates. Due to the scale size of α precipitates formed upon aging was much smaller than large primary α plates, these fine secondary α would obtain higher strength than α plates. Because the phase transformation from β to α obeys the BOR relationships $\{110\}_\beta//\{0001\}_\alpha$ and $[111]_\beta//[11\text{—}20]_\alpha$ (Ref 32). Some of dislocations would storage at the α/β phase interfaces, while the others should cross through such α/β interfaces and concentrate within α precipitates. Therefore, such fine secondary α precipitates produced higher density of α/β interfaces than large α plates, resulted in larger resistance to dislocation slipping.

The deformed microstructures consisting of α phase with different morphology and size were studied shown in Fig. 11, like α plates and fine α particles. Their characters were apparently different. The α plates showed comparable larger thickness, length and aspect ratio (> 30) but had lower number density. In contrary, the fine α particles exhibited short-rod shape, as well as smaller thickness, length and aspect ratio (< 5). Generally, the fine α particles have larger number density. After deformation, the sample with basketweave microstructure showed plenty of α plates and some α particles in nearby regions (Fig. 11a). The formation of such α particles was due to local stress concentration facilitated the grooving, boundary splitting and globularization of α plates during deformation. The microstructure in regions nearby the fracture surface is shown in Fig. 11(b), in which these α plates have been sheared off by dislocation. This suggested that the alloy with basketweave microstructure was deformed by dislocation shearing mechanism. For the samples with fine α particles microstructure, there was no apparent changes on α phase morphology during early deformation, as shown in Fig. 11(c). In regions nearby the fracture surface these fine α particles was apparently extended along the direction having 45° with the tension (Fig. 11d). The deformation behavior of fine α particles has been studied in detail before (Ref 33). In comparison with α plates, the deformation degree of fine α particles was much smaller, which explained the lower fracture elongation in samples with larger volume fraction of fine secondary α phase.

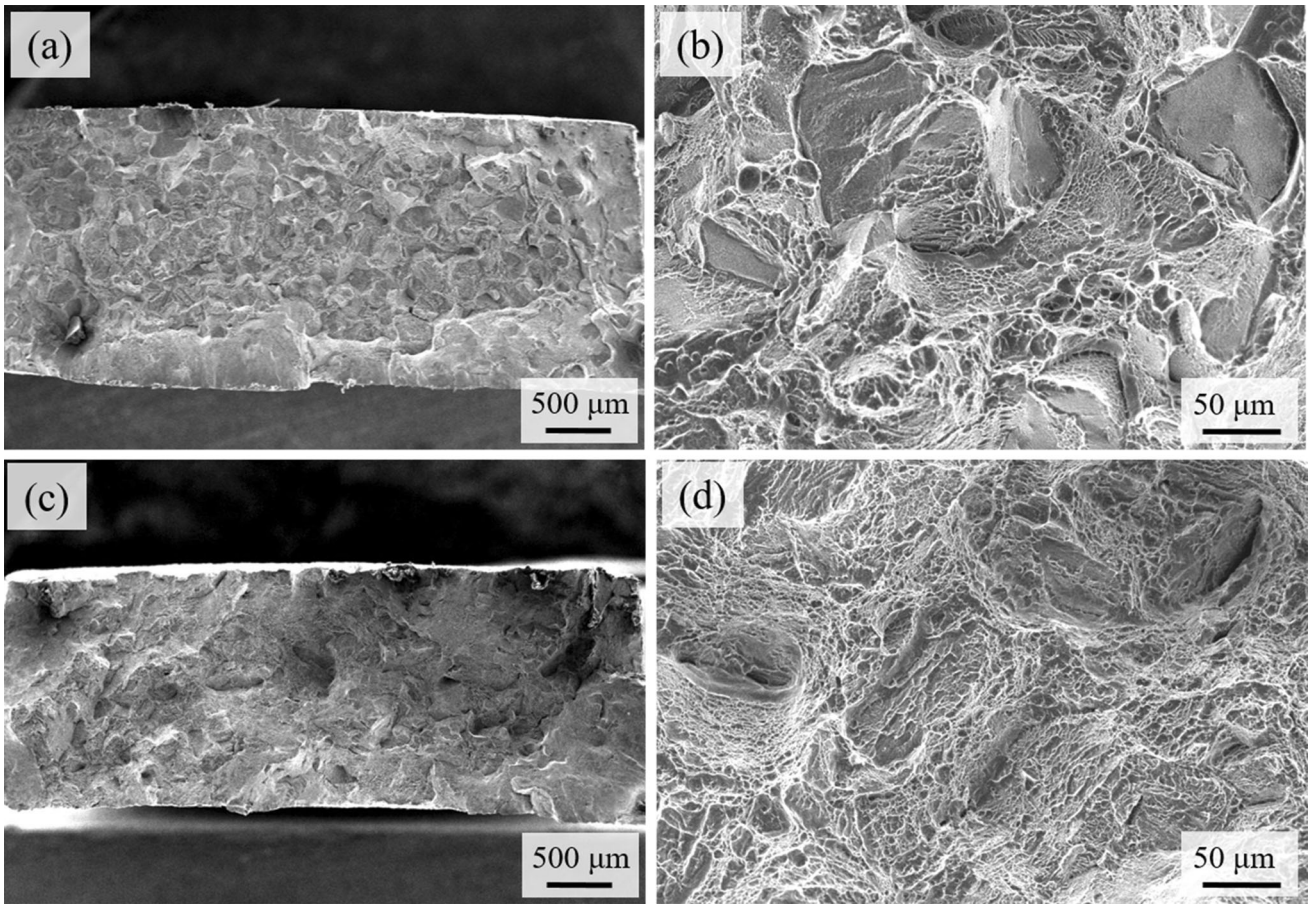

Fig. 9 Fractographs of the aged specimens when held at 800 °C (a, b) and 750 °C (c, d) at cooling rate of 10 °C/min

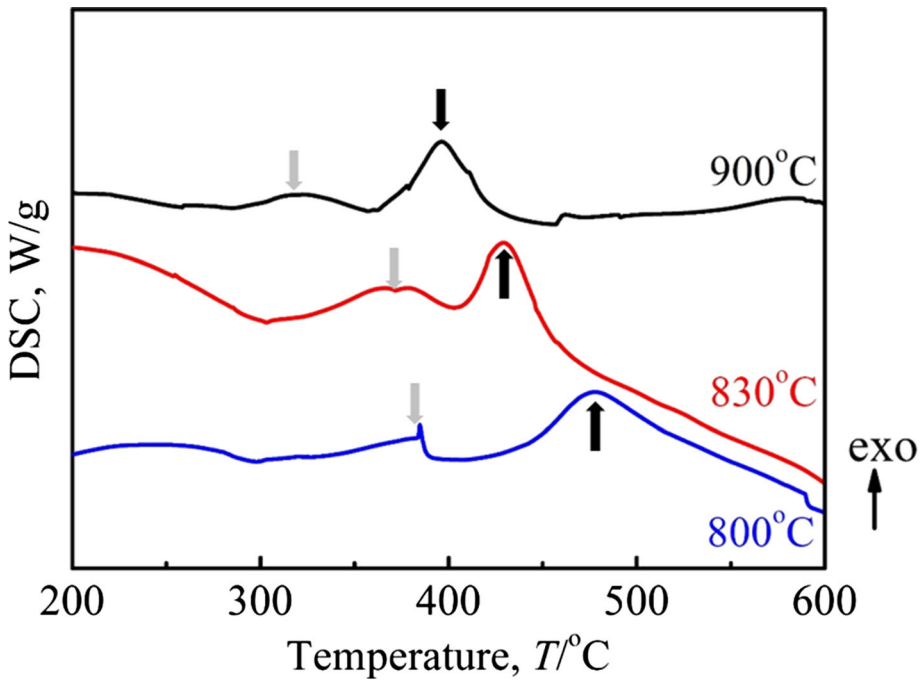

Fig. 10 DSC heat flow curves showing phase transformations during aging when the samples were solution treated at 900 °C, and those then isothermally held at 830 and 800 °C

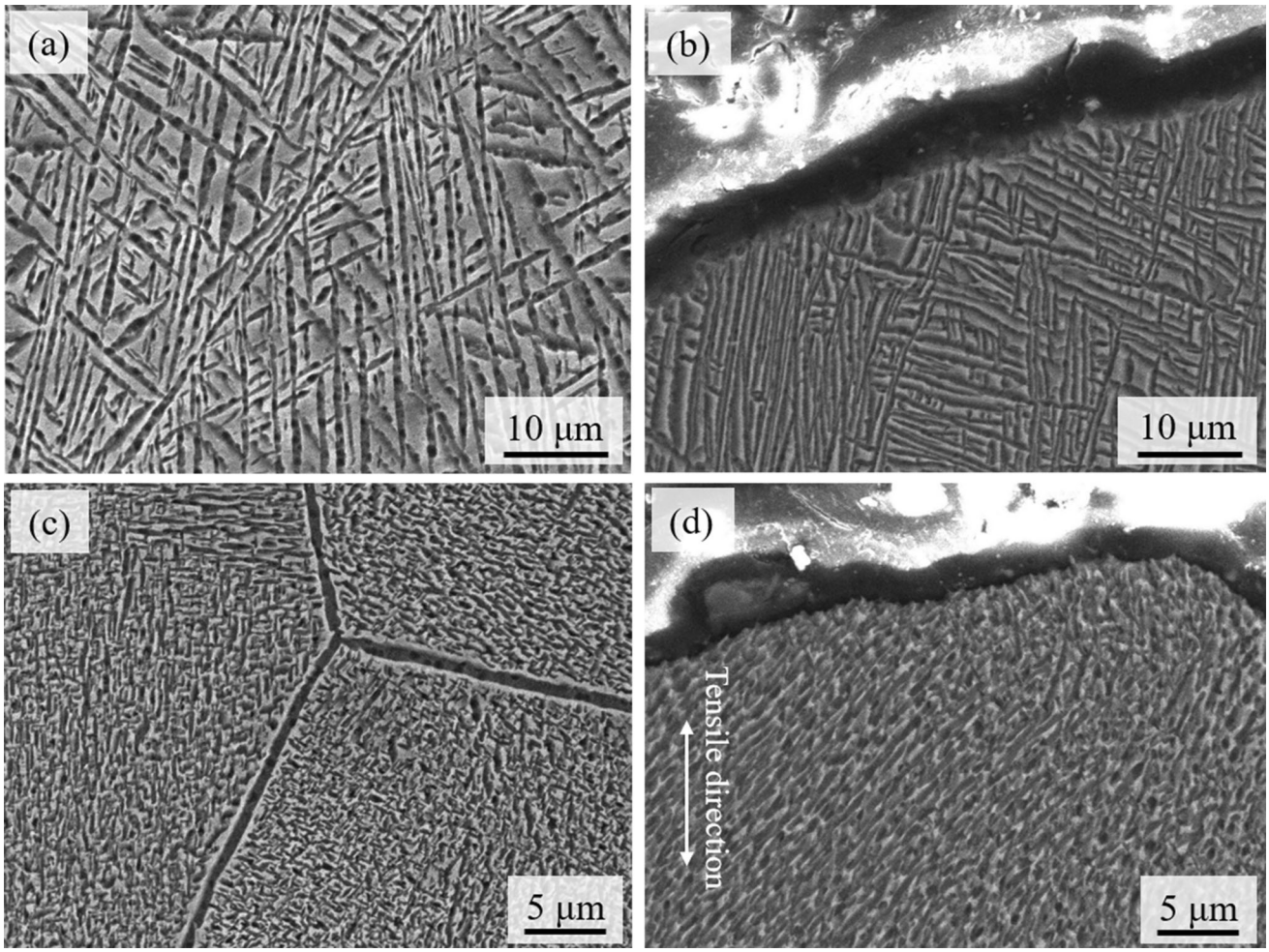

Fig. 11 SEM images showing the deformation and damage behaviors of α precipitates having different characters, (a, b) large α plates and (c, d) fine α particles

5. Conclusions

(1) The slow cooling rate and the isothermal holding temperature in isothermal solution treatment played an important role in affecting microstructure evolution and mechanical properties of Ti-5321 alloy. When the isothermal holding temperatures were higher than 750 °C, mixed microstructure consisting of α plates and fine α precipitates could be formed, otherwise basketweave microstructures were developed.

(2) The hardness difference between various cooling rates was gradually reduced with the isothermal holding temperature increasing. When the holding temperature was increased, the volume fraction of α lamellar dropped gradually, and the quantities of secondary α precipitates was increased in final aged samples. These secondary α precipitates were more efficient to strengthen alloy, because they could produce higher density of α/β interfaces impeding dislocation slipping.

(3) A balanced combination of strength and ductility was achieved after aging under the slow cooling of 10 °C/min and holding temperature of 800 °C, and the yield strength, ultimate tensile strength, elongation and area reduction were 1470 ± 17, 1497 ± 12 MPa, 4.0 ± 1 and 5.8 ± 2%, respectively.

Acknowledgments

The authors are grateful to the financial support by the National Natural Science Foundation of China (NSFC, Nos. 51671012 and 51671007), International Science and Technology Cooperation Program of China (2015DFA51430), Aeronautical Science Foundation of China (2015ZF51069) and Natural Science Foundation of Shandong Province of China (Nos. ZR2020QE026 and ZR2021ME083) to carry out this work.

Conflict of interests

The authors declare that they have no known competing financial interests or personal relationships that could have appeared to influence the work reported in this paper.

References

1. J.D. Cotton, R.D. Briggs, R.R. Boyer, S. Tamirisakandala, P. Russo et al., State of the Art in Beta Titanium Alloys for Airframe Applications, *JOM*, 2015, **67**, p 1281–1303.
2. G. Lutjering and J.C. Williams, *Titanium*, Springer, Berlin, 2007
3. R. Dong, H. Kou, Y. Zhao, X. Zhang, L. Yang et al., Morphology Characteristics of α Precipitates Related to the Crystal Defects and the Strain Accommodation of Variant Selection in a Metastable Beta Titanium Alloy, *J. Mater. Sci. Technol.*, 2021, **95**, p 1–9.
4. H. Ke, X. Zhang, J. Li, Zhou, Lian, Evolution of the Secondary α Phase Morphologies During Isothermal Heat Treatment in Ti-7333 Alloy, *J. Alloys Compd.*, 2013, **577**, p 516–522.
5. S. Wang, Y. Liang, H. Sun, X. Feng and C. Huang, Tuning the Number Density of αs Precipitates in Ti-6Al-2Sn-2Zr-3Mo-1Cr-2Nb-0.1Si Alloys for Achieving High Strength, *J. Alloys Compd.*, 2021, p 160732.
6. S.A. Mantri, D. Choudhuri, T. Alam, G.B. Viswanathan, J.M. Sosa et al., Tuning the Scale of α Precipitates in β-Titanium Alloys for Achieving High Strength, *Scr. Mater.*, 2018, **154**, p 139–144.
7. C. Wu and M. Zhan, Microstructural Evolution, Mechanical Properties and Fracture Toughness of Near β Titanium Alloy During Different Solution Plus Aging Heat Treatments, *J. Alloys Compd.*, 2019, **805**, p 1144–1160.
8. S. Shekhar, R. Sarkar, S.K. Kar and A. Bhattacharjee, Effect of Solution Treatment and Aging on Microstructure and Tensile Properties of High Strength β Titanium Alloy, Ti–5Al–5V–5Mo–3Cr, *Mater. Des.*, 2015, **66**, p 596–610.
9. Q. Zhang, J. Chen, H. Tan, X. Lin and W.D. Huang, Influence of Solution Treatment on Microstructure Evolution of TC21 Titanium Alloy with Near Equiaxed β Grains Fabricated by Laser Additive Manufacture, *J. Alloys Compd.*, 2016, **666**, p 380–386.
10. O.M. Ivasishin, P.E. Markovsky, Y.V. Matviychuk, S.L. Semiatin, C.H. Ward and S. Fox, A Comparative Study of the Mechanical Properties of High-Strength β-Titanium Alloys, *J. Alloys Compd.*, 2008, **457**, p 296–309.
11. Y. Wang, M. Hao, D. Li, P. Li, Q. Liang et al., Enhanced Mechanical Properties of Ti-5Al-5Mo-5V-3Cr-1Zr by Bimodal Lamellar Precipitate Microstructures via Two-Step Aging, *Mater. Sci. Eng. A*, 2021, p 142117.
12. N. Yumak and K. Aslantaş, A Review on Heat Treatment Efficiency in Metastable β Titanium Alloys: The Role of Treatment Process and Parameters, *J. Mater. Sci. Technol.*, 2020, **9**, p 15360–15380.
13. B. Song, W.L. Xiao, C. Ma and L. Zhou, Influence of Phase Transformation Kinetics on the Microstructure and Mechanical Properties of Near β Titanium Alloy, *Mater. Charact.*, 2019, **148**, p 224–232.
14. R. Dong, J. Li, H. Kou, J. Fan, Y. Zhao et al., ω-Assisted Refinement of α Phase and Its Effect on the Tensile Properties of a Near β Titanium Alloy, *J. Mater. Sci. Technol.*, 2020, **44**, p 24–30.
15. X. Li, X.N. Wang, K. Liu, G.H. Cao, M.B. Li et al., Hierarchical Structure and Deformation Behavior of a Novel Multicomponent β Titanium Alloy with Ultrahigh Strength, *J. Mater. Sci. Technol.*, 2022, **107**, p 227–242.
16. H. Jiang, Z.X. Du, D. Wang, T. Gong, X. Cui et al., Preparation of Multiscale α Phase by Heat Treatments and Its Effect on Tensile Properties in Metastable β Titanium Alloy Sheet, *Metals*, 2021, **11**, p 1–13.
17. C.S. Tan, Y. Fan, Q. Sun and G. Zhang, Improvement of the Crack Propagation Resistance in an α + β Titanium Alloy with a Trimodal Microstructure, *Metals*, 2020, **10**, p 1–11.
18. T.W. Xu, S.S. Zhang, F.S. Zhang, H.C. Kou and J.S. Li, Effect of ω-assisted precipitation on β → α transformation and tensile properties of Ti–15Mo–2.7Nb–3Al–0.2Si alloy, *Mater. Sci. Eng. A*, 2016, **654**, p 249–255.
19. S. Sadeghpour, S.M. Abbasi, M. Morakabati, Microstructural Evolution of a New Beta Titanium Alloy During the Beta Annealing, Slow Cooling and Aging Process. TMS 147th Annual Meeting & Exhibition Supplemental Proceedings, 2018, 829–838
20. S. Sadeghpour, S.M. Abbasi, M. Morakabati and S. Bruschi, Correlation Between α Phase Morphology and Tensile Properties of a New Beta Titanium Alloy, *Mater. Des.*, 2017, **121**, p 24–35.
21. H. Wang, Y. Zhao, Q. Zhao, S. Xin, W. Zhou et al., Microstructure Evolution and Fracture Behavior of Ti-5Al-3Mo-3V-2Zr-2Cr-1Nb-1Fe Alloy During BASCA Heat Treatments, *Mater. Charact.*, 2021, **174**, p 110975.
22. L. Ren, W. Xiao, H. Chang, Y. Zhao, C. Ma and L. Zhou, Microstructural Tailoring and Mechanical Properties of a Multi-alloyed near β Titanium Alloy Ti-5321 with Various Heat Treatment, *Mater. Sci. Eng. A*, 2018, **711**, p 553–561.
23. Y.Q. Zhao, C.L. Ma, H. Chang and L. Zhou, New High Strength and High Toughness Titanium Alloy with 1200 MPa, *Materials China*, 2016, **35**, p 914–917.
24. B. Song, Y. Chen, W. Xiao et al., Formation of Intermediate Phases and Their Influences on the Microstructure of High Strength Near-β Titanium Alloy, *Mater. Sci. Eng. A*, 2020, **793**, p 139886.
25. T. Li, M. Lai, A. Kostka et al., Composition of the Nanosized Orthorhombic O′ Phase and Its Direct Transformation to Fine α During Ageing in Metastable β-Ti Alloys, *Scr. Mater.*, 2019, **170**, p 183–188.
26. Bo. Song, YuFu. Wenlong Xiao et al., Role of Nanosized Intermediate Phases on a Precipitation in a High-Strength Near β Titanium Alloy, *Mater. Lett.*, 2020, **275**, p 128147.
27. Q. Liang, D. Wang, Y. Zheng et al., Shuffle-Nanodomain Regulated Strain Glass Transition in Ti-24Nb-4Zr-8Sn Alloy, *Acta Mater.*, 2020, **186**, p 415–424.
28. Y. Zheng, R.E.A. Williams and H.L. Fraser, Characterization of a Previously Unidentified Ordered Orthorhombic Metastable Phase in Ti-5Al-5Mo -5V-3Cr, *Scr. Mater.*, 2016, **113**, p 202–205.
29. F. Chen, G. Xu, K. Zhou et al., Isochronal and Isothermal Phase Transformation in β + α Acicular Ti–55531, *J. Mater. Sci.*, 2020, **55**, p 3073–3091.
30. Y. Liu, S.C.V. Lim, C. Ding, A. Huang and M. Weyland, Unravelling the Competitive Effect of Microstructural Features on the Fracture Toughness and Tensile Properties of Near Beta Titanium Alloys, *J. Mater. Sci. Technol.*, 2022, **97**, p 101–112.
31. X. Zhu, Q. Fan, D. Wang, H. Gong, Y. Gao et al., Deformation mechanism of fine structure and its quantitative relationship with quasi-static mechanical properties in near β-type Ti-4.5Mo-5.1Al-1.8Zr-1.1Sn-2.5Cr −29Zn alloy, *Prog. Natural Sci. Mater. Int.*, 2021, **31**, p 742–748.
32. Y. Zheng, R.E.A. Williams, G.B. Viswanathan, W.A.T. Clark and H.L. Fraser, Determination of the Structure of α-β Interfaces in Metastable β-Ti Alloys, *Acta Mater.*, 2018, **150**, p 25–39.
33. W. Kou, Q. Sun, L. Xiao and J. Sun, Coupling Effect of Second Phase and Phase Interface on Deformation Behaviours in Microscale Ti-55531 Pillars, *J. Alloys Compd.*, 2020, **820**, p 153421.